ISSN (Print) 1226-1750
ISSN (Online) 2233-6656
Journal of Magnetics 18(2), 135-141 (2013) http://dx.doi.org/10.4283/JMAG.2013.18.2.135

Efficient Fault Detection Method for a Degaussing Coil System Based on an Analytical Sensitivity Formula

Nak-Sun Choi[1], Dong-Wook Kim[1], Chang-Seob Yang[2], Hyun-Ju Chung[2], Heung-Geun Kim[1], and Dong-Hun Kim[1]*

[1]*Department of Electrical Engineering, Kyungpook National University, Daegu 702-701, Korea*
[2]*The 6th R&D Institute-2, Agency for Defense Development, Changwon 645-600, Korea*

(Received 4 March 2013, Received in final form 23 May 2013, Accepted 24 May 2013)

This paper proposes an efficient fault detection method for onboard degaussing coils which are installed to minimize underwater magnetic fields due to the ferromagnetic hull. To achieve this, the method basically uses field signals measured at specific magnetic treatment facilities instead of time-consuming numerical field solutions in a three-dimensional analysis space. In addition, an analytical design sensitivity formula and the linear property of degaussing coil fields is being exploited for detecting fault coil positions and assessing individual degaussing coil currents. Such peculiar features make it possible to yield fast and accurate results on the fault detection of degaussing coils. For foreseeable fault conditions, the proposed method is tested with a model ship equipped with 20 degaussing coils.

Keywords : diagnosis, electromagnetics, inverse problem, design sensitivity

1. Introduction

In the earth's magnetic field, the ferromagnetic hull of a ship is magnetized and accordingly it induces underwater magnetic fields around the ship. To mitigate such field for ship's safety, the vessels are usually equipped with several tens of onboard degaussing coils consisting of longitudinal (L), athwartship (A) and vertical (V) coils (refer to Fig. 1) [1-4]. The principle of the degaussing technique is to generate degaussing coil field of which the magnitude is same as that of the induced field due to the hull but two fields (i.e. induced field and degaussing field) have opposite directions with each other. Several research works relating to optimizing degaussing coil currents have been reported. Either sampling-based or sensitivity-based optimization method was successfully applied to reducing the underwater magnetic fields as little as possible [4]. Meanwhile, from the view of the maintenance point, the diagnosis of the degaussing coils is another important issue in the degaussing technique because the abnormal currents flowing through the degaussing coils abruptly deteriorate the degaussing performances. It means that the underwater magnetic field signals under such abnormal conditions become much larger and consequently it is easily liable to expose vessels to fatal hazards such as magnetic mines or torpedoes. However, it is currently difficult to find published articles regarding this topic in our community of electromagnetics.

This paper presents an efficient fault detection method for onboard degaussing coils which basically uses measurement data of underwater magnetic field signals instead of time-consuming numerical field solutions (e.g. three-dimensional finite element method with a very fine mesh model). In order to achieve this, the experimental components for extracting underwater field signals of the ship are briefly introduced. The method exploits an analytical design sensitivity formula with respect to the magnetomotive forces (mmf) of degaussing coil and the linear property of degaussing coil fields. The aforementioned features make it possible to yield fast and accurate results on the fault detection of degaussing coils. For several fault conditions, the proposed method is tested with a model ship equipped with 20 degaussing coils.

2. Underwater Field Signals of a Model Ship

In this section, the disposition of degaussing coils and experimental setup for extracting underwater field signals under the model ship is briefly explained. The difference of field signals between normal and abnormal degaussing

©The Korean Magnetics Society. All rights reserved.
*Corresponding author: Tel: +82-53-950-5603
Fax: +82-53-950-5603, e-mail: dh29kim@ee.knu.ac.kr

© 2013 Journal of Magnetics

conditions is illustrated and then two representative failure modes of degaussing coils are being defined.

2.1. Experimental Setup

A ship made of steel plate with a length of 200 m, width of 30 m and height of 20 m is considered for a test model. Usually, the ship is equipped with three kinds of degaussing coils, namely L coil, V coil and A coil, as shown in Fig. 1 where the arrows denote the positive directions of degaussing coil currents. The role of the coils is to cancel the magnetic field results corresponding to the sum of the induced magnetic field (IM) and the permanent magnetic field (PM). While IM is generated due to the induced magnetization on the ferromagnetic hull under the earth magnetic field, PM is created by the residual permanent magnetization on the hull after a deperming process [5]. The resultant field can be decomposed into three field components on the basis of the ship's heading as: longitudinal magnetic fields (LM), athwartship magnetic fields (AM) and vertical magnetic fields (VM) [4, 5]. The three-type coils of L, V and A, are properly installed in order so that their composite field waveforms coincide with those of the three-type resultant fields, respectively. Therefore, after a normal degaussing process where optimum degaussing currents are allotted to the individual coils, the maximum value of the final fields (i.e. degaussed fields) can be reduced by more than 90% of the resultant field before the process.

Fig. 2 shows a schematic magnetic treatment system for measuring underwater magnetic fields before and after the degaussing process. To obtain field signals, tri-axial magnetic sensors with high precision are placed at a specified depth under the keel.

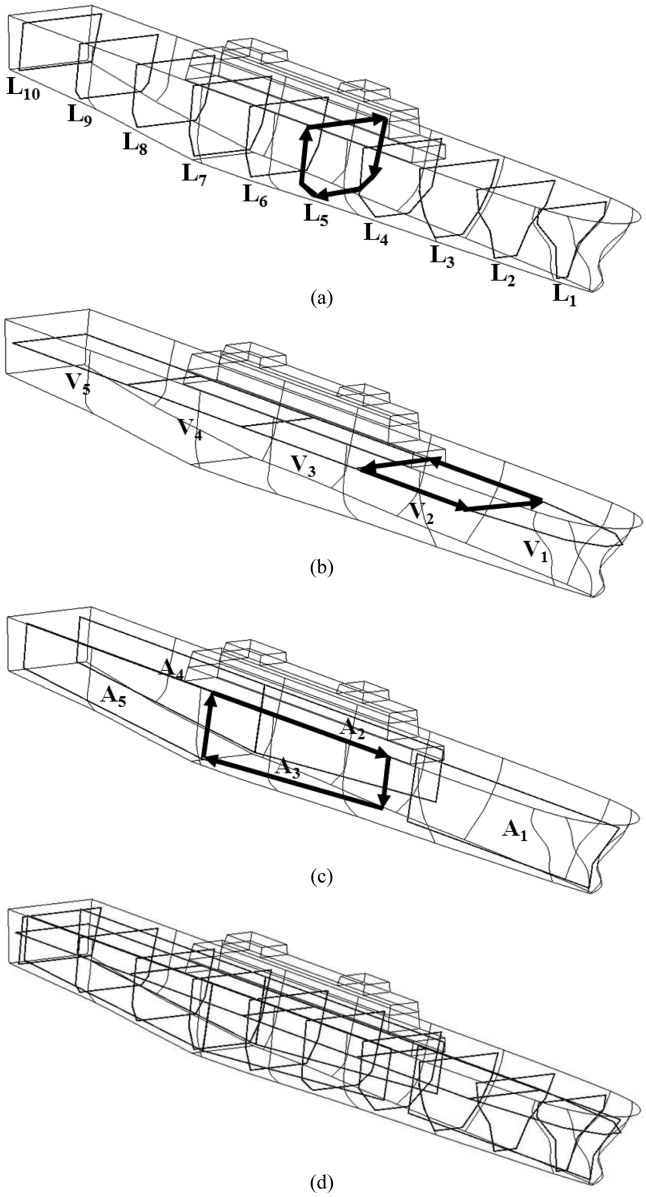

Fig. 1. Schematic of onboard degaussing coils: (a) L coil array, (b) V coil array, (c) A coil array, (d) Assembly coils.

2.2. Underwater Field Signals

The field distribution from measured signals along the measurement line is illustrated in Fig. 2 where field waveforms between normal and abnormal degaussing conditions are compared with each other. While the circled symbols suggest the degaussed field is in a normal condition, the squared ones correspond to one of the observable fault field signals. The abnormal degaussing conditions can be classified into two representative failure modes:

Mode I) More than one coil do not work due to a breakdown in either power supply units or coil connections,

Mode II) Insufficient or excessive currents out of optimum degaussing currents flow through more than one coil.

In practice, the experiment is carried out as the ship slowly moves twice along each intercardinal direction (i.e. north-east heading and south-west heading) against the sensor at a standstill as in Fig. 3. The time-dependent field signals are transformed into a space-dependent one and then the three-type field components, LM, AM and VM, are easily extracted through the simple arithmetic means, respectively [5]. Such field signal extraction is called an

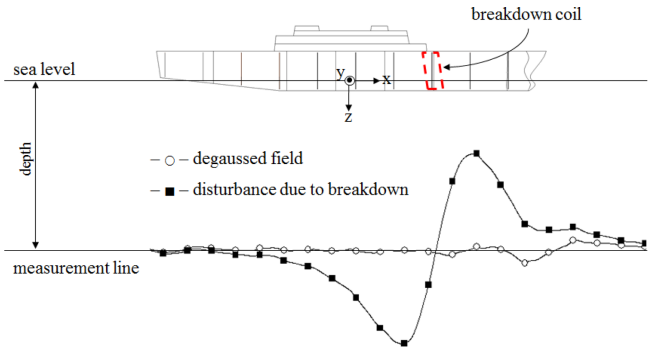

Fig. 2. (Color online) Illustration of experimental setup for measuring underwater field signals.

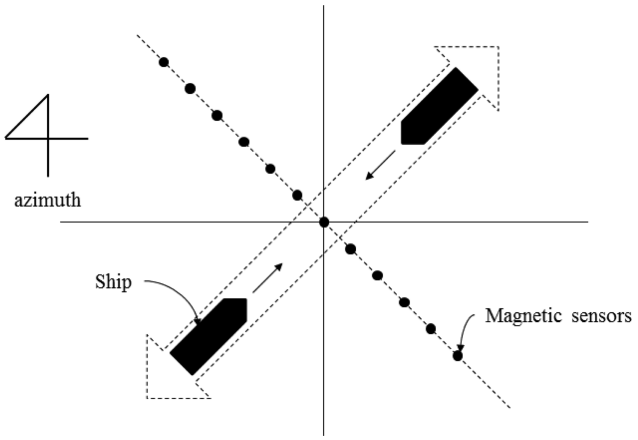

Fig. 3. Sectional plane of intercardinal movement techniques.

intercardinal movement technique (IMT). After the IMT process, it is revealed that two decomposed fields, LM and AM, include only IM components, respectively, but the rest of VM contains both field components consisting of IM and PM. For degaussing maintenance, IMT has to be executed separately twice for the same ship at a time interval for a few years. In the proposed method, the first measured data right after the degaussing process is used as reference field values to identify the failure modes and to detect faulty coil positions.

3. Proposed Fault Detection Method

For accurate and fast fault detections of the degaussing coils, the linearity of degaussing fields and an analytical mmf sensitivity formula are introduced. Then, the implementation for the proposed fault detection method are described.

3.1. Linearity of Degaussing Fields

The mmf imposed on each degaussing coil generates underwater magnetic fields (i.e. degaussing fields) and, subsequently, the ferromagnetic hull is locally magnetized around the coil. The locally induced magnetization on the hull results in a shielding effect which mitigates the degaussing field approximately up to 20%. This effect depends on the relative location and shape between the coil and the hull. Therefore, to accurately tune the degaussing coil currents without experimental field data of individual coils, a time-consuming numerical analysis has to be executed along with a very fine mesh model of the hull within a three-dimensional analysis space. However, if the aim is just to diagnose degaussing coils, there is no necessity to obtain such highly accurate field solutions of individual coils. Such big difference in field signals usually appears between normal and the abnormal degaussing conditions and it can be detected by means of pure fields generated by the coils themselves without shielding effects of the hull. In such

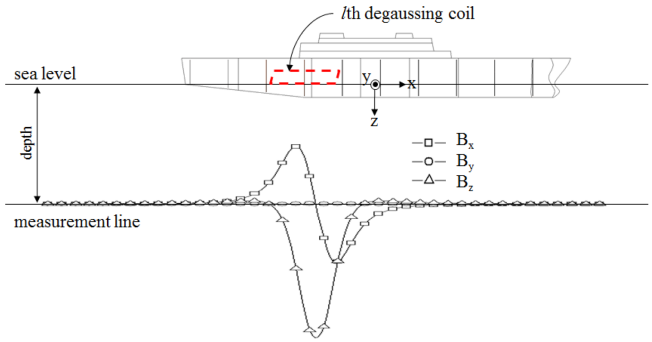

Fig. 4. (Color online) Illustration of degaussing field components due to the *l*th degaussing coil.

cases, the field linearity is applied to predict degaussing fields of individual coils at any mmf values given. When all the degaussing coils do not work, individual coil fields are calculated from a simple integral equation describing the Biot-Savart law as successively feeding a reference mmf value $\Im_R$ to each coil. For instant, Fig. 4 shows the orthogonal components of reference degaussing field B_j on the measurement line when the *l*th degaussing coil is activated with $\Im_R$. After all, degaussing field B created by the *l*th coil at any mmf value $\Im$ is easily estimated by (1).

$$\mathbf{B} = \mathbf{B}_j \frac{\Im}{\Im_R} \quad j = 1,\ldots np \tag{1}$$

where *np* is the number of measuring points.

3.2. Analytical Sensitivity Formula

To identify the failure modes and to detect faulty coil positions, the objective function is defined on the measuring line at a depth of 20 m under the keel as depicted in Fig. 2:

$$\text{minimize } F = \sum_{i=1}^{3}\sum_{j=1}^{np}\sum_{k=1}^{nl} ((B_{ij}^{nor} - B_{ij}^{abnor}) - B_{ij}^{k})^2 \tag{2}$$

where B_{ij}^{nor} is degaussed field data under the normal degaussing condition, B_{ij}^{abnor} is field data including the disturbance under the abnormal degaussing condition, the subscripts, *i* and *j*, are the directional component and measurement point, respectively, the superscript *k* is coil numbering, and *nl* denotes the number of degaussing coils installed. The field difference between B_{ij}^{nor} and B_{ij}^{abnor} includes only IM signals because PM component does not change under both the normal and abnormal conditions. The function *F* is set to find a faulty coil position and deviation amount of individual coils out of optimum mmf values that are well-established through the degaussing process.

In order to search for an optimum of the inverse problem (2), an analytical mmf sensitivity formula, which gives the

first-order gradient information of an objective function, is utilized herein. In general, the sensitivity formula is derived through somewhat cumbersome mathematical procedures such as the governing Maxwell's equation, augmented objective function, and adjoint variable method [6-9]. Detailed procedure of the sensitivity formula for magnetostatic inverse problems has already been developed in [8] and [9]; the only concern right now, is to combine the sensitivity formula with the objective function (2).

Final mathematical expression of the sensitivity formula for the objective function F with respect to the coil mmf is given by (3).

$$\frac{dF}{d\mathbf{p}} = \int_{\Omega} \left(\frac{\partial \Im}{\partial \mathbf{p}}\right) \cdot \lambda \, d\Omega \tag{3}$$

where $\mathbf{p}$ is the system parameter, Ω is the cross-section of the coil, and λ denotes the Lagrange multiplier interpreted as the adjoint vector potential. That is, it is a field solution of the adjoint system which is the counterpart of the primary/original system. At the nkth iterative design during the optimization process, the pseudosource of the adjoint system is defined by differentiating (2) with respect to B_{ij}^{k}.

$$M_j^{nk} = -2\sum_{i=1}^{3}\sum_{j=1}^{np}\sum_{k=1}^{nl} ((B_{ij}^{nor} - B_{ij}^{abnor}) - B_{ij}^{k}) \tag{4}$$

where M_j^{nk} corresponds to the pseudosource located at the jth measurement point, which can be interpreted as virtual magnetic dipole moment. It should be noticed that the degaussing coils have to be removed in the adjoint system. After all, the adjoint vector potential for the lth coil is calculated by

$$\lambda^{nk} = \sum_{j=1}^{np} \mathbf{M}_j^{nk} \times \nabla\left(\frac{1}{r}\right) \tag{5}$$

where r is the distance from the pseudosource to the coil position.

3.3. Implementation

To simplify numerical implementation, the coil mmf is forced to be a linear function of the system parameter $\mathbf{p}$ in (3) [10, 11]. A general-purpose optimizer, called DOT based on the Broydon–Fletcher–Goldfarb–Shanno (BFGS) algorithm in [12], is adopted to accelerate the convergence of the objective function. The coil mmf values are initially set to zero. The iterative design process involves the following steps:

1) Prepare two kinds of underwater field data measured after the degaussing process and after a maintenance period, the three-type field components, LM, AM and VM, are extracted.

2) Check the differences in each component between the two field data and only stop the fault detecting process blow when all differences in the three components are relatively small as compared with a certain allowance value.

3) Define an objective function and design variables with a specified field component and its corresponding coil type when the difference is above the allowance value.

4) Assess the objective function (2) and then calculate the adjoint source (4).

5) Compute the adjoint variable λ from (5) and sensitivity value for each coil with (3), respectively.

6) Update individual coil mmf value $\Im$ ($\Im_l^{nk+1} = \Im_l^{nk} + \alpha\Delta\mathbf{p}$) at the nkth iteration, where l and α is the lth degaussing coil and relaxation factor, respectively.

7) Check convergence and go to step 4 if unsatisfactory.

4. Case Study

For foreseeable faulty conditions, the proposed method is tested with a model ship equipped with 20 degaussing coils as shown in Fig. 1. To unify the coordinate system used, the x axis in Fig. 2 is set to the North Magnetic Pole. For an easy way to verify the method, the finite element analysis (FEA) solutions are treated as measured field data. Using a commercial FEA software packages, MagNet VII [13], the ship was divided into more than 5 million of tetrahedral elements and the relative permeability of the hull was set to be 320. It took more than 50 minutes to obtain a FEA solution for only one fault simulation with a desktop computer equipped with an Intel Core i7 CPU of 3.2 GHz.

Compared with reference field profiles in a normal degaussing condition, underwater field distributions in two failure modes are presented in Fig. 5 where a maximum field value of each case is set to be unity: Mode I has a L_2 coil breakdown and Mode II has insufficient mmf values flowing into L_3 and L_7 coils (refer to Fig. 1). In Mode II, the mmf values allotted to the two coils were forced to reduce by one third of the normal degaussing ones, respectively. It is observed that abnormal coil currents cause considerably big differences in field distributions between the normal and abnormal degaussing conditions. According to the above assumptions, the objective function (2) was defined with the LM component and 10 design variables of L coils. The mmf values of L coils for the two failure modes were assessed by the proposed fault detecting method. Even though more than 60 iterative designs were required in each failure mode, it took less than 3 seconds for the convergence of the objective function. Fig. 6 shows normalized mmf histograms where the slash bars mean the deviation amount of individual coils from the normal degassing mmf values denoted with white bars. From the results, it can be easily deduced that the L_2 coil breakdown occurred in Fig. 6(a) and L_3 and L_7 coils are short of coil mmf values by nearly 33% with respect to the normal ones,

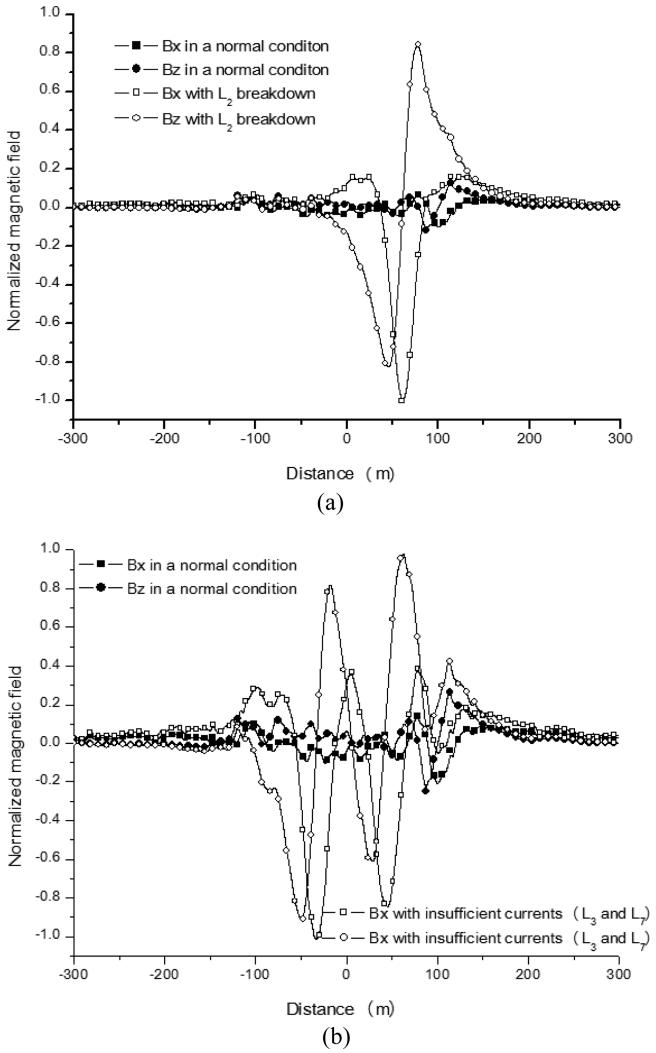

Fig. 5. Normalized field distributions between normal and abnormal degaussing conditions where a maximum field value in each case is set to be unity: (a) Breakdown of L_2 coil, (b) Insufficient currents of L_3 and L_7.

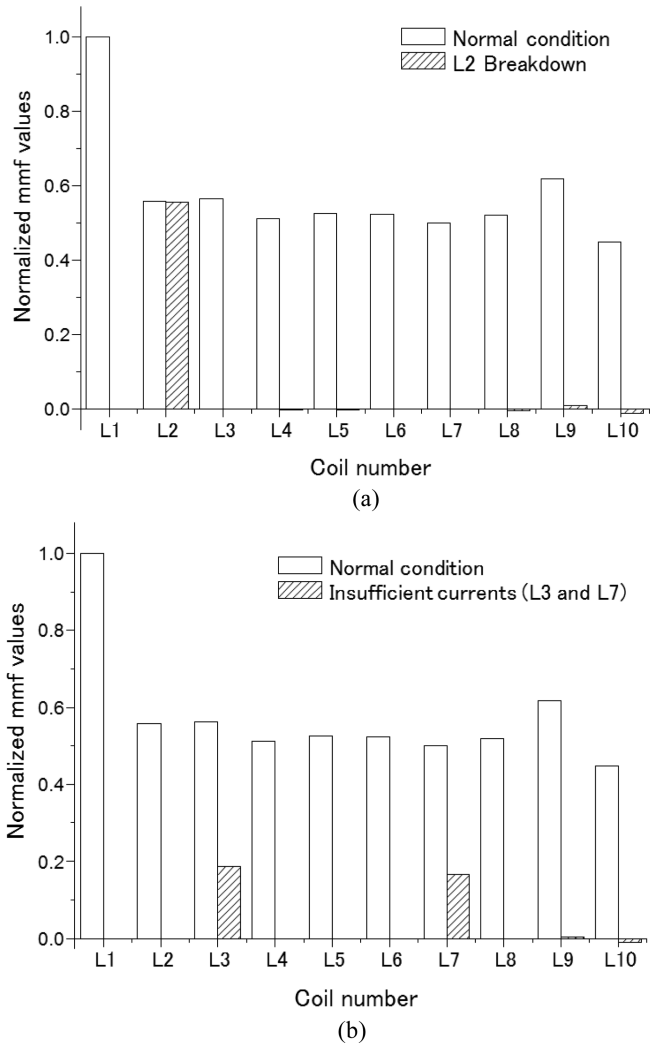

Fig. 6. Normalized mmf values between normal and abnormal degaussing conditions where the slash bars correspond to the deviation amount from normal degaussing mmf values: (a) Breakdown of L_2 coil, (b) Insufficient currents of L_3 and L_7.

respectively. In the two histograms, relatively tiny slash bars are observed specifically at L_9 and L_{10} coils. It results from the fact that the proposed method basically uses not highly accurate numerical field solutions but rather the simple field integral equation and linear property of degaussing fields without the shielding effects of the hull. However, it is obvious that the tiny bars do not affect the decision making process in detecting faulty coil positions and assessing the state of the individual coil mmf.

Various fault conditions of degaussing coils are thoroughly investigated in Tables 1 and 2 where possible combination of the failure mode, breakdown coil and failure option are being considered. The notations used in the failure option means that F is a full breakdown, and II-a and II-b are to feed one-third insufficient or excessive mmf values to normal degaussing ones, respectively. The asterisk of II-a* in Table 1 denotes that coil current flows in the opposite direction of normal degaussing one. Each column except the first one in the tables represents one of the faulty conditions simulated in advance. After executing the proposed fault detection method case by case, the digits in individual columns correspond to the results which are individually normalized with respect to normal degaussing mmf values. The bold number in the column corresponds to the deviated mmf amount and fault coil position. The plus/minus sign gives information on whether the mmf of a detected faulty coil is insufficient or excessive to the normal one. In Table 1, four different faulty conditions were tested with L coils. For instance, the second column corresponds to Mode I where two adjacent coils of L_2 and L_3 are broken down. From the result, it is observed that two meaningful numbers, 0.990 and 1.003, are found at the two breakdown coils. The numbers means

Table 1. Fault current indicators for L coils under foreseeable breakdown conditions.

Failure mode	Mode I	Mode I		Mode II	Mode I+II	
Breakdown coil	L_2	L_2	L_3	L_{10}	L_3	L_7
Failure option	F	F	F	II-a*	F	II-b
L_1	0.001	0.006		0.004	0.000	
L_2	**0.995**	**0.990**		-0.010	0.002	
L_3	0.001	**1.003**		0.004	**0.994**	
L_4	-0.002	-0.003		-0.005	0.003	
L_5	-0.002	0.002		0.001	-0.003	
L_6	-0.001	-0.002		-0.009	0.001	
L_7	0.002	0.004		0.011	**-0.333**	
L_8	-0.010	-0.007		-0.034	-0.006	
L_9	0.013	0.008		0.041	0.010	
L_{10}	-0.024	-0.016		**1.730**	-0.020	

L_2 and L_3 are short of the mmf values by 99.0% and 100.3%, respectively. In the third column, a special faulty condition is considered where L_{10} has an insufficient mmf value and also its current direction is opposite to the normal one (i.e. the normalized mmf value of –0.667 is imposed on L_{10}). The result implies that the calculated mmf of 1.730 has to be added to the abnormal mmf of –0.667. Theoretically, the sum of two values, 1.730 and –0.667, must become one. The difference, 0.063, is a relatively small but it is the largest error in the results. That is because the proposed method does not take into account the shielding effect of the hull which would be the biggest influence on L_1 and L_{10} among the installed coils. The last column simulates the composite fault consisting of Mode I and Mode II, where L_3 is broken down and L_7 has an excessive mmf value. Two numbers, 0.994 and –0.333, mean that L_3 is short of the mmf by 99.4% and L_7 has an excessive mmf by 33.3%. Meanwhile, three different faulty conditions were additionally tested with the three-type coils in Table 2. To deal with the three-type fault coils, three different objective functions must be defined successively along with the specific field components and corresponding coils of L, A and V. Afterwards, the objective functions are solved one by one. Among the three fault cases, the third column belongs to the composite fault where A_4 coil is broken down, V_3 has an excessive mmf and L_9 coil has an insufficient mmf. The result shows faulty coil positions and deviated mmf values accurately.

5. Conclusion

In this paper, an efficient fault detection method for onboard degaussing coils in a ship is proposed and tested with a model ship equipped with 20 degaussing coils. The method basically uses field signals measured at specific magnetic treatment facilities, an analytical design sensitivity formula and the linear property of degaussing coil fields. Through various fault simulations, it is verified that the method yields fast and accurate results on the faulty coil positions and its mmf state.

Acknowledgment

This work was supported by the Power Generation & Electricity Delivery of Korea Institute of Energy Technology Evaluation and Planning (KETEP) grant funded by the Korea government Ministry of Knowledge Economy (No. 20111020400260).

Table 2. Fault current indicators for three-type coils under foreseeable breakdown conditions.

Failure mode	Mode I			Mode II			Mode I+II		
Breakdown coil	V_3	A_4	L_6	V_3	L_3	L_7	V_3	A_4	L_9
Failure option	F	F	F	II-b	II-a	II-a	II-b	F	II-a
V_1, V_2	-0.007, 0.019			-0.022, 0.029			-0.022, 0.029		
V_3	**0.975**			**-0.310**			**-0.310**		
V_4, V_5	0.032, -0.044			0.014, -0.015			0.014, -0.015		
A_1, A_2, A_3	0.008, 0.075, -0.053			0.000, 0.000, 0.000			0.008, 0.075, -0.053		
A_4	**0.990**			0.000			**0.990**		
A_5	0.003			0.000			0.003		
L_1,L_2	-0.005, 0.001			0.000, -0.001			-0.001, -0.001		
L_3	0.000			**0.331**			0.000		
L_4, L_5	-0.004, 0.002			0.000, -0.003			-0.002, 0.000		
L_6	**0.997**			0.000			-0.004		
L_7	0.004			**0.333**			0.004		
L_8	-0.007			-0.004			-0.012		
L_9	0.012			0.007			**0.347**		
L_{10}	-0.018			-0.022			-0.028		

References

[1] R. Donati and J. P. Le Cadre, IEE Proc. Radar Sonar Navig. **149**, 221 (2002).
[2] O. Chadebec, J. Coulomb, J. Bongiraud, G. Cauffet, and P. Thiec, IEEE Trans. Magn. **38**, 1005 (2002).
[3] O. Chadebec, J. Coulomb, G. Cauffet, and J. Bongiraud, IEEE Trans. Magn. **39**, 1634 (2003).
[4] H. Liu and Z. Ma, Proc. Int. Conf. Mechatronics and Automation 3133 (2007).
[5] C. Yang, K. Lee, G. Jung. H. Chung, J. Park, and D. Kim, J. Appl. Phys. **103**, 905 (2008).
[6] J. H. Lee, *et al*., IEEE Trans. Appl. Supercond. **14**, 1906 (2004).
[7] M. Minakami, IEEE Trans. Appl. Supercond. **14**, 940 (2004).
[8] N. Choi, G. Jeung, C. Yang, H. Chung, and D. Kim, IEEE Trans. Appl. Supercond. **42**, 4904504 (2012).
[9] N. Choi, G. Jeung, S. Jung, C. Yang, H. Chung, and D. Kim, IEEE Trans. Magn. **48**, 419 (2012).
[10] K. Lee, H. Choi, W. Nah, I. Park, J. Kang, J. Joo, J. Byun, Y. Kwon, M. Sohn, and S. Kim, IEEE Trans. Magn. **45**, 1478 (2009).
[11] D. Kim, J. Sykulski, and D. Lowther, IEEE Trans. Magn. **41**, 1752 (2005).
[12] DOT User Manual, Vanderplaats Research & Development Inc., Colorado Springs, USA (2001).
[13] MagNet User's Manual, Infolytica Corporation, Quebec, Canada (2008).